Original Article

JCBFM

Journal of Cerebral Blood Flow & Metabolism
2016, Vol. 36(1) 264–274

DOI: 10.1038/jcbfm.2015.64
jcbfm.sagepub.com

SAGE

Blood pressure and sodium: Association with MRI markers in cerebral small vessel disease

Anna K Heye[1,*], Michael J Thrippleton[1,*], Francesca M Chappell[1], Maria del C Valdés Hernández[1], Paul A Armitage[1,2], Stephen D Makin[1], Susana Muñoz Maniega[1], Eleni Sakka[1], Peter W Flatman[3], Martin S Dennis[1] and Joanna M Wardlaw[1]

Abstract

Dietary salt intake and hypertension are associated with increased risk of cardiovascular disease including stroke. We aimed to explore the influence of these factors, together with plasma sodium concentration, in cerebral small vessel disease (SVD). In all, 264 patients with nondisabling cortical or lacunar stroke were recruited. Patients were questioned about their salt intake and plasma sodium concentration was measured; brain tissue volume and white-matter hyperintensity (WMH) load were measured using structural magnetic resonance imaging (MRI) while diffusion tensor MRI and dynamic contrast-enhanced MRI were acquired to assess underlying tissue integrity. An index of added salt intake ($P = 0.021$), pulse pressure ($P = 0.036$), and diagnosis of hypertension ($P = 0.0093$) were positively associated with increased WMH, while plasma sodium concentration was associated with brain volume ($P = 0.019$) but not with WMH volume. These results are consistent with previous findings that raised blood pressure is associated with WMH burden and raise the possibility of an independent role for dietary salt in the development of cerebral SVD.

Keywords

Blood pressure, salt, sodium, small vessel disease, white-matter hyperintensities

Received 15 January 2015; Revised 13 March 2015; Accepted 13 March 2015

Introduction

Cerebral small vessel disease (SVD) accounts for 20% to 25% of strokes and causes cognitive impairment, disability, and dementia. The pathogenesis of SVD is poorly understood but hypertension and other vascular risk factors have been identified. Previous work in our group revealed associations between blood pressure and white-matter hyperintensity (WMH) burden and between blood pressure and previsible white-matter damage assessed by diffusion tensor imaging.[1,2]

The influence of dietary salt intake on stroke incidence and mortality is well known[3] but may be only partly mediated by its effect on blood pressure.[4] Plasma sodium concentration is assumed to be tightly regulated but there is some evidence to suggest that even small variations can affect physical and mental health in the elderly population.[5,6] The role of dietary and plasma sodium in cerebral SVD is unclear.

In this work, we assessed a cohort of patients with recent nondisabling stroke and exhibiting a spectrum of SVD severity. We performed magnetic resonance

[1]Neuroimaging Sciences, University of Edinburgh, Edinburgh, UK
[2]Department of Cardiovascular Science, University of Sheffield, Sheffield, UK
[3]Centre for Integrative Physiology, University of Edinburgh, Edinburgh, UK
[*]These authors contributed equally to this work

Corresponding author:
Joanna M Wardlaw, Brain Research Imaging Centre, Neuroimaging Sciences, University of Edinburgh, Western General Hospital, Crewe Road, Edinburgh EH4 2XU, UK.
Email: joanna.wardlaw@ed.ac.uk

imaging (MRI) scans to assess WMH volume, brain tissue volume, diffusion tensor MRI (DT-MRI) measures of tissue integrity, and T1-weighted imaging of contrast uptake. Blood pressure, an index of added dietary salt intake, and plasma sodium concentration were assessed and tested for associations with imaging findings.

Materials and methods

Participants

Participants were 264 adult patients who presented to our in- and out-patient stroke service. We recruited consecutive patients with first clinically evident nondisabling lacunar or mild cortical ischemic stroke, including those with diabetes, hypertension, and other vascular risk factors. We excluded patients with unstable hypertension or diabetes, other neurologic disorders and major medical conditions including renal failure that would preclude use of intravenous gadolinium contrast agents. We excluded patients unable to give consent, with contraindications to MRI or intravenous contrast, who had hemorrhagic stroke or those whose symptoms resolved within 24 hours (i.e., transient ischemic attack). The study was approved by the Lothian Research Ethics Committee (REC 09/81101/54) and the NHS Lothian R&D Office (2009/W/NEU/14) and conducted according to the principles expressed in the Declaration of Helsinki. All patients gave written informed consent.

Clinical data, diet and smoking history, WMH volume, brain tissue volume, and DT-MRI were obtained at presentation. Participants returned approximately 1 to 3 months after presentation for dynamic contrast-enhanced MRI (DCE-MRI), the delay being to avoid acute effects of the stroke on the local blood–brain barrier.

Clinical and Laboratory Measurements

On presentation, a clinician trained in stroke obtained the clinical details of the presenting stroke and determined the clinical stroke subtype (lacunar and cortical) using the Oxfordshire Community Stroke Project (OCSP) classification.[7] The same clinical researcher also recorded age, demographic details, past medical history of hypertension, previous stroke, previous transient ischemic attack, ischemic heart disease, peripheral vascular disease, diabetes mellitus, atrial fibrillation, hypercholesterolemia, heart failure, smoking and alcohol use, as well as all medications used and obtained blood biochemistry, brain MRI and other stroke investigations. We defined hypertension as blood pressure of 140/90 mmHg or greater on presentation or a previous diagnosis; smokers were defined as currently smoking or having given up within the previous 12 months and nonsmokers as having never smoked or having given up more than 12 months previously.

An experienced neuroradiologist assessed acute stroke subtype (lacunar or cortical) on MR diffusion-weighted imaging (generated from DT-MRI), fluid-attenuated inversion recovery (FLAIR), T2 and T1-weighted diagnostic imaging. Acute lacunar infarcts were required to be less than 20 mm in maximum axial diameter and in the deep white or gray matter (GM) of the cerebral hemispheres or brainstem. Infarcts involving the cortex, or subcortical infarcts larger than 20 mm diameter (i.e., a large striatocapsular infarct) were classed as 'cortical', likely to be due to large artery atherothromboembolism. All scans and clinical details were then reviewed by an expert panel of neurologists, stroke physicians, and neuroradiologists to establish the final stroke subtype using all clinical and imaging information. If no lesion was present on imaging, then the stroke was classified based on the clinical findings alone using the Bamford classification.[7]

We measured systolic and diastolic blood pressure (SBP and DBP, respectively) from the brachial artery in the stroke clinic or stroke ward using hospital blood pressure devices, which were checked and maintained by technical staff. Pulse pressure (PP) and mean arterial pressure (MAP) were calculated as SBP−DBP and DBP, respectively. Plasma sodium concentration was measured from blood samples taken during clinic assessment and measured in the NHS Lothian Biochemistry Department.

Participants were also asked to describe their addition of salt to food during cooking and at the dining table using the following salt intake score: 1 = always, 2 = often, 3 = occasionally, 4 = rarely, and 5 = never; the mean of the two scores was subtracted from 6 to give an ordinal categorical variable in the range of 1 (minimum use of salt) to 5 (maximum use of salt) for use in statistical analyses.

Magnetic Resonance Imaging

Magnetic resonance imaging was performed with a 1.5 Tesla MRI scanner (Signa HDxt, General Electric, Milwaukee, WI, USA) using an 8-channel phased-array head coil. Diagnostic MRI was acquired at presentation, including axial T2-weighted (T2W; repetition time (TR)/echo time (TE) = 6,000/90 ms, 24 × 24 cm field of view (FoV), 384 × 384 Propeller acquisition, 1.5 averages, 28 × 5 mm slices, 1 mm slice gap), axial FLAIR (TR/TE/inversion time (TI) = 9,000/153/2,200 ms, 24 × 24 cm FoV, 384 × 224 acquisition matrix, 28 × 5 mm slices, 1 mm slice gap), axial GRE (gradient echo; TR/TE = 800/15 ms, 20° flip angle, 24 × 18 cm

FoV, 384×168 acquisition matrix, 2 averages, 28×5 mm slices, 1 mm slice gap) and sagittal 3D T1-weighted imaging (T1W; inversion recovery-prepared SPGR (spoiled gradient echo) TR/TE/TI = 7.3/2.9/500 ms, 8° flip angle, 330×214.5 cm FoV, 256×146 acquisition matrix, 100×1.8 mm slices) and DT-MRI (single-shot echo-planar imaging with 30 diffusion directions ($b = 1{,}000$ s/mm^2) and $2 \times b_0$ acquisitions, TR/TE = 7,700/82 ms, 24×24 cm FoV, 128×128 acquisition matrix, 28×5 mm slices, 1 mm slice gap). The DCE-MRI was performed between 1 and 3 months after first presentation (median 38, interquartile range (31,54) days) and consisted of 20 consecutive 3D T1W SPGR acquisitions (TR/TE = 8.2/3.1 ms, 12° flip angle, 24×24 cm FoV, 256×192 acquisition matrix, 42×4 mm slices, 73 seconds acquisition time) with a total acquisition time of approximately 24 minutes, initiated simultaneously with an intravenous bolus injection of 0.1 mmol/kg gadoterate meglumine (Gd-DOTA, Dotarem, Guerbet, France). Two additional SPGR acquisitions were obtained before contrast administration with flip angles of 2° and 12°, respectively for calculation of the precontrast longitudinal relaxation time $T_{1,0}$.

Image Processing and Analysis

Preprocessing. Magnetic resonance images were converted from DICOM to Analyze 7.5 format. Structural and DCE-MRI images were aligned to the precontrast T1W image using rigid-body registration (FSL-FLIRT[8]); for participants who did not receive DCE-MRI, images were instead coregistered to the T2W image.

Tissue segmentation. The FLAIR and GRE images were processed using in-house software ('MCMxxxVI'[9]) to extract WMH in the brain parenchyma; these were manually refined and, separately, old stroke lesions or index stroke lesions were manually outlined using Analyze 11.0 (AnalyzeDirect, Stilwell, KS, USA). White-matter hyperintensity was identified as punctate or diffuse areas in the white matter and deep GM of the cerebral hemispheres or in the brainstem that were 3 mm or larger in diameter and hyperintense with respect to normal-appearing white matter and GM on T2W and FLAIR images; some hypointensity on T1W MRI was allowed as long as not less intense than cerebrospinal fluid (CSF). White-matter hyperintensity included 'dirty' or ill-defined diffuse hyperintensities with varying and erratic intensity patterns emerging from the lateral ventricle wall[10,11] provided such regions had outstanding intensity differences with respect to the normal-appearing white matter (NAWM) identified on T1W images. Index stroke lesions were defined as the hyperintense regions identified on the diffusion-weighted image generated from the DT-MRI scan including any corresponding signal changes on FLAIR, T2W, and T1W images, associated with swelling or lack of *ex vacuo* effect, that followed a vascular territory. Old stroke lesions were wedge-shaped hyperintense regions on the FLAIR or T2W images, and hypointense on the T1W image including cortex and/or subcortical tissues, with or without cavitation, and with *ex vacuo* effect reflecting tissue loss. The NAWM masks were generated using MCMxxxVI as described in Valdés Hernández et al.[12] Subcortical GM masks were generated automatically by a software pipeline that used FSL-SUSAN[13] for noise reduction, an age-relevant brain template,[14] FSL-FLIRT for aligning the template to each image data set, and FSL-FIRST[15] for extracting the subcortical structures, followed by manual boundary correction. To minimize any residual contamination of the subcortical GM, the mask was eroded by one voxel. An example of MR images and segmentation masks is shown in Figure 1.

Brain tissue volume. Intracranial volume (ICV), defined as contents within the inner skull table including brain tissue, CSF, veins, and dura, and limited inferiorly by the tip of the odontoid peg at the foramen magnum, was extracted using the GRE image and the Object Extraction Tool in Analyze 11.0, followed by manual editing. Nonbrain tissue (CSF, venous sinuses, and meninges) was extracted using MCMxxxVI. The volume of the resulting 'nonbrain' binary masks was subtracted from the ICV to provide a measure of total brain tissue volume. For statistical analysis, the brain tissue volume as a percentage of ICV (%BTV) and the WMH volume as a percentage of ICV (%WMH) were also calculated.

Diffusion tensor magnetic resonance imaging processing. The DTI images were processed using in-house software, which removed bulk motion and eddy current induced distortions using FSL FLIRT[8] and generated a directionally averaged diffusion-weighted image, mean diffusivity (MD), and fractional anisotropy (FA) parametric images using standard methods based on multivariate linear regression. For each data set nonlinear registration[16] was used to align the tissue masks in the structural space (T2W) with the parametric maps in the diffusion space using the NiftyReg tool (http://sourceforge.net/projects/niftyreg/) applied using TractoR software (http://www.tractor-mri.org.uk/diffusion-processing) to obtain the transformation between the brain extracted structural T2W image and the b_0 diffusion volume. To avoid partial volume averaging with CSF due to registration inaccuracies, the CSF mask was dilated by one voxel in each direction and

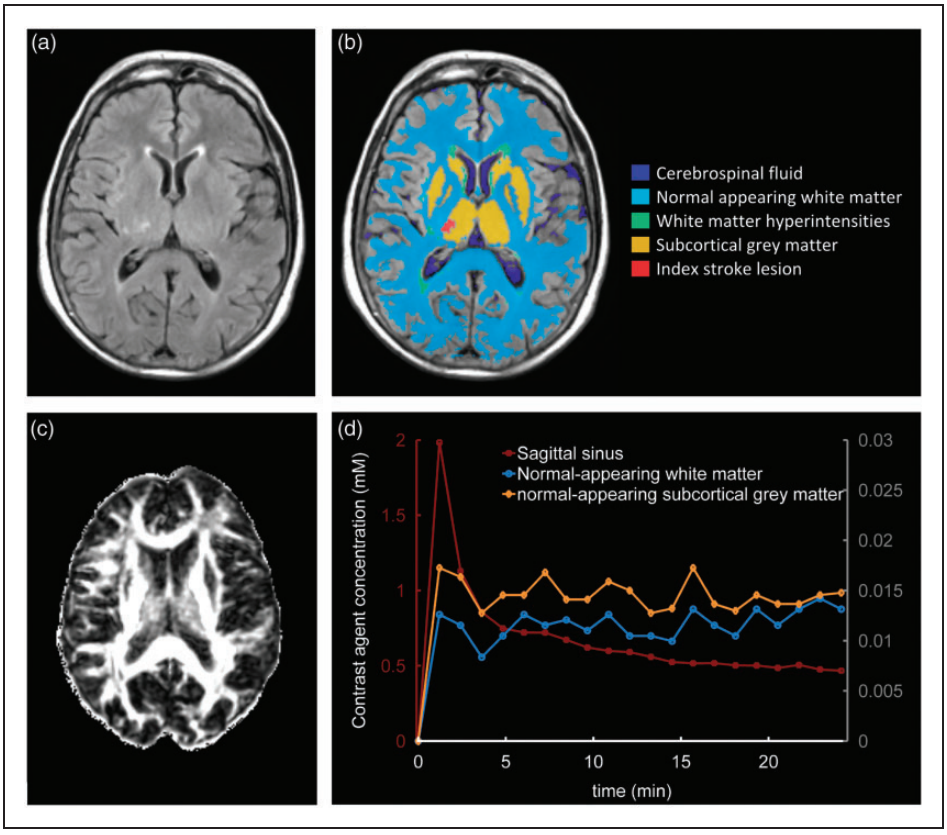

Figure 1. Representative magnetic resonance imaging (MRI) data and tissue segmentation. (A) Fluid-attenuated inversion recovery (FLAIR) image, (B) tissue masks superimposed on FLAIR image, (C) fractional anisotropy map, (D) contrast agent concentration curves obtained from dynamic contrast-enhanced MRI (DCE-MRI); y-axes scales for the sagittal sinus plasma concentration and normal-appearing tissue concentration curves are shown on the left and the right, respectively.

then subtracted from the NAWM, WMH, and subcortical GM masks in the diffusion space. Median MD and FA were extracted for NAWM and subcortical GM in each patient.

Dynamic contrast-enhanced magnetic resonance imaging. Median signal intensities for normal-appearing subcortical GM and white matter masks were extracted from the coregistered precontrast and postcontrast T1W images. A vascular input function was also determined by manual selection of a voxel in the superior sagittal sinus, using a slice proximal to the basal ganglia structures and the lateral ventricles. This voxel was chosen to provide a high peak signal enhancement and smooth variation during the DCE-MRI time course and was chosen independently by two observers; where the observers selected different voxels, the voxel with the highest peak enhancement was chosen unless the signal curve was significantly noisier (a noise estimate was calculated as the sum of squared differences between the signal curve and a fitted biexponential curve). $T_{1,0}$ was calculated using the median signal intensities in the two precontrast images with flip angles 2° and 12° and used to derive time-concentration curves for each tissue as described in Armitage et al.;[17] contrast agent concentration in the sagittal sinus was converted to plasma concentration using the factor 1/(1–Hct) and the most recent available hematocrit measurement in the patient's clinical record (if no hematocrit measurement was available ($n = 3$) we assumed Hct = 0.45). To semiquantitatively assess contrast uptake in tissue, we calculated the normalized area under curve (nAUC) defined as the area under the tissue concentration curve divided by the area under the superior sagittal sinus plasma concentration curve.

Statistical Analysis

Descriptive statistics in the text are given as mean ± standard deviation. Regressions were assessed by examination of the differences between the data and model predictions, and collinearity by variance inflation factors using SPSS version 19 (IBM Corp., Armonk, NY, USA) and Matlab (MathWorks, Inc., Natick, MA, USA). Predictors of %WMH and %BTV were investigated using multiple linear

regression models with correction for age, smoking status, stroke subtype, and additional factors given in the text and tables. Residuals for the %WMH model were not approximately normally distributed; to correct for this, the transformed outcome variable $\ln(0.005 + \%\text{WMH})$ was regressed instead. Subcortical GM MD (units $10^{-6}\,\text{mm}^2/\text{s}$) was also transformed to $\ln(-700 + \text{MD})$ for this reason.

Results

Subjects

A total of 264 subjects were recruited into the study with mean age 66.9 ± 11.8 years and a ratio of 45:55 for diagnosis of lacunar-to-cortical stroke; 39% of patients were smokers and 72% had hypertension (Table 1). Reasons for exclusion are shown in Figure 2. After withdrawals and rejection of imaging data on quality grounds, DT-MRI and DCE-MRI data suitable for analysis were obtained in 262 and 201 patients, respectively.

White-Matter Hyperintensity and Brain Tissue Volume

Mean WMH volume as a percentage of ICV was $1.5 \pm 1.6\%$ with a positively skewed distribution. Pulse pressure ($\beta = 0.0092$/mm Hg, $P = 0.036$) and a diagnosis of hypertension ($\beta = 0.46$, $P = 0.0093$) were significant predictors of increased WMH volume as a percentage of ICV with correction for age, stroke subtype, and smoking status (Table 2 and Figure 3). Repetition of the analysis with replacement of PP and MAP with DBP and SBP showed that SBP but not DBP was positively associated with transformed %WMH ($\beta = 0.0079$/mm Hg, $P = 0.040$). Salt intake score was also positively associated with WMH volume ($\beta = 0.14$, $P = 0.021$; Figure 3); further analyses using the separate scores for cooking and table salt usage were consistent with this finding ($\beta = -0.11/-0.067$; $P = 0.020/0.18$ for cooking/table salt—note that the coefficient sign change is expected, since the combined score was inverted). Regression analysis of brain tissue volume (mean: $71 \pm 5\%$ of ICV) with the same covariates revealed a positive association between plasma sodium concentration and %BTV corresponding to an increase in brain tissue volume of 2% ICV per 10 mmol/L sodium ($P = 0.019$). Age was the most significant factor in the analyses of both %WMH and %BTV ($P < 0.0001$).

Diffusion Tensor Magnetic Resonance Imaging

The DT-MRI data were obtained in 262 subjects (DT-MRI data for two subjects were rejected due to failure of the nonlinear image registration). Mean diffusivity was distributed with mean values of 801 ± 52 and $787 \pm 32 \times 10^{-6}\,\text{mm}^2/\text{s}$ in subcortical GM and NAWM, respectively, with corresponding FA of 0.234 ± 0.021 and 0.256 ± 0.022. The influence of blood pressure, added salt intake, and plasma sodium concentration on these variables was modelled with correction for smoking, stroke subtype, and age, as well as normalized WMH volume to account for SVD severity (Table 3). Plasma sodium concentration was negatively associated with MD in NAWM ($\beta = -1.2 \times 10^{-6}\,(\text{mm}^2\,\text{L})/(\text{s mmol})$; $P = 0.011$) and FA in subcortical GM ($\beta = -0.9 \times 10^{-3}\,\text{L/mmol}$; $P = 0.021$). Salt intake score was negatively associated with FA in subcortical GM ($\beta = -3.4 \times 10^{-3}\,\text{L/mmol}$; $P = 0.0012$); additional analyses using the separate scores for salt usage during cooking and at the table were consistent with this finding ($\beta = 2.0/2.5$; $P = 0.016/0.0052$ for cooking/table salt). In WM, there were

Table 1. Descriptive statistics for demographic, clinical, and imaging variables including DT-MRI and DCE-MRI parameters in normal-appearing white matter and subcortical gray matter.

Parameter	N	*Mean (s.d.)*
Age (years)	264	66.9 (11.8)
Sex (% female)	264	42
Stroke subtype (% lacunar)	264	45
Hypertension (%)	264	72
Smoker[a] (%)	262	39
Diabetes (%)	264	11
Pulse pressure (mm Hg)	264	63 (20)
Mean arterial pressure (mm Hg)	264	103 (15)
Salt intake score	250	2.7 (1.3)
Plasma sodium concentration (mmol/L)	260	139 (3)
Structural MRI		
%WMH (%)	264	1.5 (1.6)
%BTV (%)	264	71 (5)
DT-MRI		
MD ($10^{-6}\,\text{mm}^2/\text{s}$)		
GM	262	801 (52)
NAWM	262	787 (32)
FA		
GM	262	0.234 (0.021)
NAWM	262	0.256 (0.022)
DCE-MRI		
nAUC (10^{-3})		
GM	201	16.8 (4.3)
NAWM	201	9.9 (3.7)

Abbreviations: BTV, brain tissue volume; DCE-MRI, dynamic contrast-enhanced MRI; DT-MRI, diffusion tensor MRI; FA, fractional anisotropy; GM, gray matter; MD, mean diffusivity; MRI, magnetic resonance imaging; nAUC, normalized area under curve; NAWM, normal-appearing white matter. [a]Currently smoking or had given up within the previous 12 months.

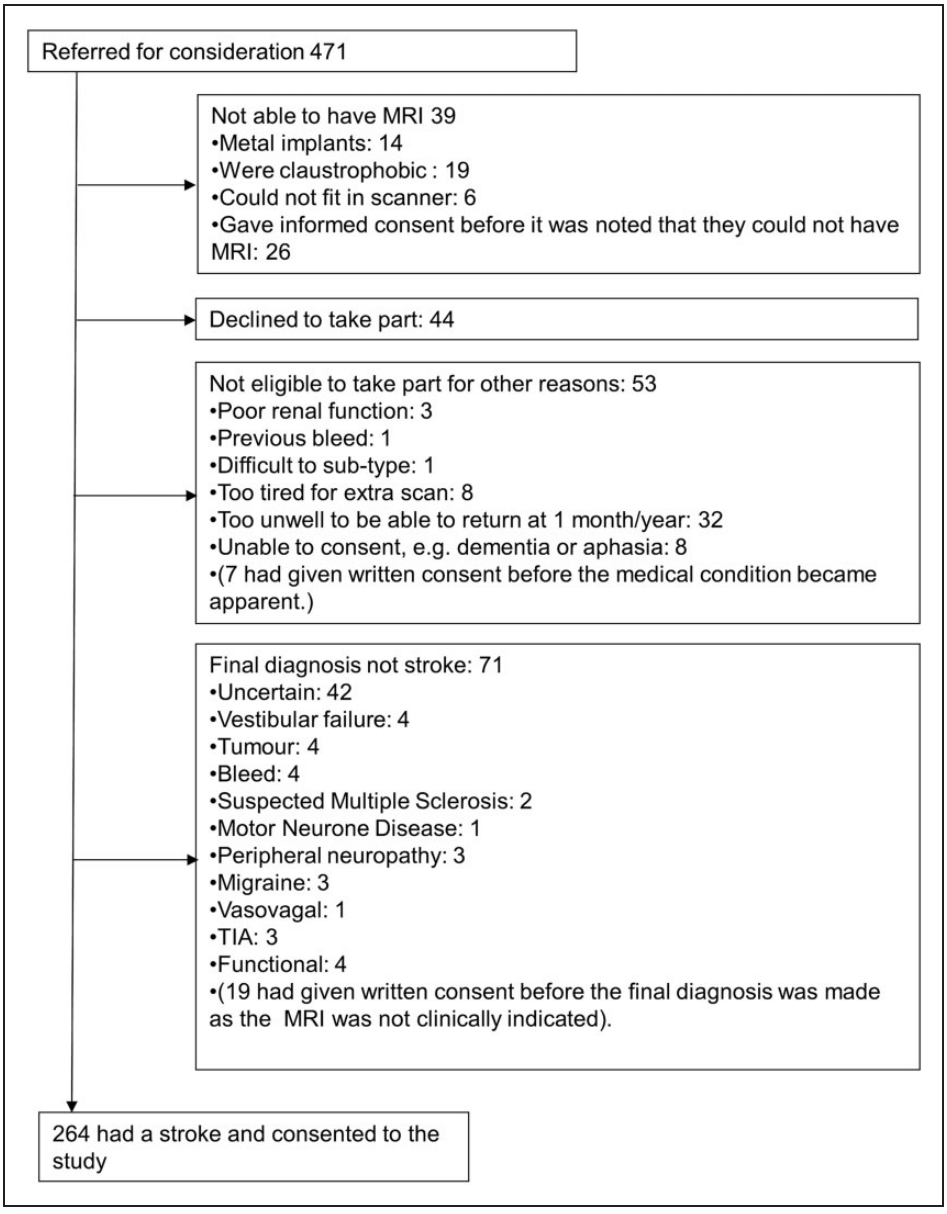

Figure 2. Flow chart showing recruitment to the Mild Stroke Study 2. MRI, magnetic resonance imaging; TIA, transient ischemic attack.

corresponding trends for reduced FA with increasing salt score ($\beta = -1.3 \times 10^{-3}$; $P = 0.19$) and lower plasma sodium ($\beta = 0.62 \times 10^{-3}$ L/mmol; $P = 0.090$) but these were not significant at the two-tailed 5% type 1 error level.

Dynamic Contrast-Enhanced Magnetic Resonance Imaging

Of the 264 patients recruited, 56 did not undergo DCE-MRI at 1-month follow-up due to decline in renal function (3), being too unwell (7), lack of venous access (4), and declining to have the scan (42). Of the 208 patients that underwent DCE-MRI, data suitable for analysis was obtained in 201 (data for seven subjects were rejected due to 'tissueing' of contrast, technical faults during the scan or unacceptable data quality caused by patient movement). The DCE-MRI parameters were modelled using the same covariates as for DT-MRI data (Table 4). Plasma sodium concentration was positively associated with nAUC in NAWM ($\beta = 0.18 \times 10^{-3}$; $P = 0.019$) but blood pressure, hypertension, and salt intake score were not significant predictors. The most significant covariate in these analyses was age, which was negatively associated with nAUC in both NAWM and subcortical GM ($P < 0.0001$).

Table 2. Multiple linear regression analysis of %WMH and %BTV.

	ln(0.005 + %WMH)		*%BTV*	
	β *(95% CI)*	*P*	β *(95% CI)*	*P*
PP (mm Hg)	0.0092 (0.00059, 0.018)	0.036	−0.022 (−0.054, 0.011)	0.20
MAP (mm Hg)	−0.0037 (−0.015, 0.0073)	0.51	0.013 (−0.029, 0.055)	0.55
Hypertension	0.46 (0.11, 0.81)	0.0093	−0.68 (−2.0, 0.65)	0.31
Salt intake score	0.14 (0.021, 0.25)	0.021	0.26 (−0.19, 0.70)	0.26
Plasma sodium (mmol/L)	−0.029 (−0.072, 0.014)	0.18	0.20 (0.033, 0.36)	0.019
Smoking	0.31 (−0.0033, 0.63)	0.052	−1.2 (−2.4, 0.039)	0.058
Stroke subtype (cortical = 0, lacunar = 1)	0.27 (−0.023, 0.57)	0.070	−0.40 (−1.5, 0.73)	0.49
Age (years)	0.053 (0.039, 0.067)	<0.0001	−0.25 (−0.30, −0.20)	<0.0001

Abbreviations: BTV, brain tissue volume; CI, confidence interval; PP, pulse pressure; MAP, mean arterial pressure; WMH, white-matter hyperintensity.

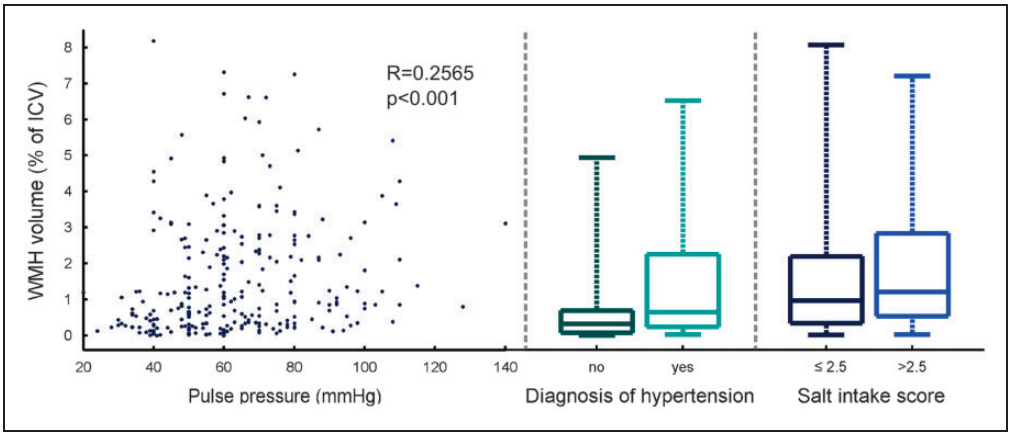

Figure 3. Relationship between white-matter hyperintensity (WMH) volume and pulse pressure (PP), diagnosis of hypertension, and salt intake score. The association between WMH volume and PP (Spearman's $R = 0.26$, $P < 0.001$) survived correction for age and all other factors listed in Table 2. ICV, Intracranial volume.

Discussion

Our finding that arterial blood pressure is associated with increased WMH volume is broadly consistent with the results of previous studies[1,2,18–21] and with the hypothesis that sustained pressure elevation and pressure fluctuations in the small cerebral vessels result in microvascular damage.[22] The independent association with clinical diagnosis of hypertension, additional to that of BP, likely reflects the historical effect of blood pressure elevation on vasculature and end organs in addition to that at the time of the study. Others have shown that WMH volume is also predicted by increased large artery stiffness, which may be one cause of increased pressure fluctuations in the small cerebral vessels.[23,24]

A novel finding of this study is that routinely adding more salt to food, which likely increases overall dietary salt intake in addition to the amounts of salt already present in food, is associated with greater WMH volume. There was also a highly significant negative association between the salt intake score and FA in normal-appearing subcortical GM, suggestive of 'previsible' reduced tissue integrity.[25] The interactions between salt intake, blood pressure, and cerebrovascular disease are not fully understood: it is widely accepted that sodium intake increases blood pressure[26] and that hypertension leads to cardiovascular disease including stroke[27,28] and there is indirect evidence to support the beneficial effects of reducing the salt intake on the incidence of cardiovascular disease.[28,29] Furthermore, epidemiologic studies indicate that salt intake is associated with increased risk of stroke and cardiovascular disease independently of blood pressure.[4,30,31] Our findings, which are corrected for blood pressure (both PP and MAP), hypertension, and age (as much as one can), suggest this might also be the case in cerebral SVD. Studies in the literature addressing the

Table 3. Multiple linear regression analysis of DT-MRI measurements in normal-appearing white matter and subcortical gray matter.

	$ln(-700 + MD_{GM}\ [10^{-6}\ mm^2/s])$		$MD_{NAWM}\ (10^{-6}\ mm^2/s)$		$FA_{GM}\ (10^{-3})$		$FA_{NAWM}\ (10^{-3})$	
	β (95% CI)	P	β (95% CI)	P	β (95% CI)	P	β (95% CI)	P
PP (mm Hg)	0.00079 (−0.0018, 0.0033)	0.54	0.16 (−0.021, 0.34)	0.083	0.056 (−0.095, 0.21)	0.47	−0.030 (−0.17, 0.11)	0.68
MAP (mm Hg)	0.0020 (−0.0013, 0.0052)	0.24	−0.14 (−0.38, 0.090)	0.23	−0.094 (−0.29, 0.10)	0.34	−0.041 (−0.22, 0.14)	0.66
Hypertension	0.046 (−0.058, 0.15)	0.39	0.64 (−6.7, 8.0)	0.86	−3.7 (−9.8, 2.4)	0.23	−2.1 (−7.9, 3.7)	0.48
Salt intake score	0.013 (−0.022, 0.048)	0.46	0.54 (−1.9, 3.0)	0.66	−3.4 (−5.5, −1.4)	0.0012	−1.3 (−3.2, 0.63)	0.19
Plasma sodium (mmol/L)	−0.0027 (−0.015, 0.010)	0.68	−1.2 (−2.1, −0.28)	0.011	−0.90 (−1.7, −0.14)	0.021	0.62 (−0.096, 1.3)	0.090
Smoking	0.016 (−0.078, 0.11)	0.74	3.8 (−2.9, 10.)	0.27	2.0 (−3.6, 7.6)	0.48	−1.5 (−6.8, 3.7)	0.57
Stroke subtype (cortical = 0, lacunar = 1)	0.096 (0.0079, 0.18)	0.033	0.60 (−5.7, 6.9)	0.85	−9.8 (−15., −4.5)	0.00029	−0.047 (−5.0, 4.9)	0.98
Age (years)	0.014 (0.0095, 0.018)	<0.0001	1.2 (0.89, 1.5)	<0.0001	0.088 (−0.18, 0.35)	0.51	−0.53 (−0.77, −0.28)	<0.0001
%WMH (%)	0.15 (0.12, 0.18)	<0.0001	4.9 (2.8, 7.0)	<0.0001	−2.3 (−4.0, −0.56)	0.0097	−4.5 (−6.1, −2.9)	<0.0001

Abbreviations: CI, confidence interval; DT-MRI, diffusion tensor MRI; MD, mean diffusivity; FA, fractional anisotropy; GM, gray matter; MAP, mean arterial pressure; NAWM, normal-appearing white matter; PP, pulse pressure; WMH, white-matter hyperintensity.

role of sodium in SVD are lacking and the pathophysiologic mechanism of any harm is unclear. A possible direct effect of salt on the endothelium, in addition to any effect via elevated BP, might account for the increased stroke risk due to salt beyond that accounted for by hypertension alone: for example, salt-sensitive (versus salt-resistant) hypertension is associated with peripheral endothelial dysfunction[32] which, if also present in the brain, might account for the dynamic cerebral and systemic endothelial dysfunction seen in several studies of SVD[33] and the increased level of WMH seen here. However, although the linear model used here fitted our data well, the significance of salt intake score as an independent predictor of WMH could also be influenced by complex nonlinear interactions between salt intake, blood pressure, and vascular disease, which become steeper with advancing age, in hypertensives and high salt intake.[28]

In contrast to dietary sodium consumption, plasma sodium concentration did not predict WMH volume but was associated with brain tissue volume, corresponding to an increase of 2% of ICV per 10 mmol/L sodium. Lower plasma sodium was also associated with increased MD in NAWM and increased FA in subcortical GM. The explanations for these associations are unknown and should be explored in future studies. Changes in brain volume may occur after acute changes in osmolality, but are thought to be temporary and rapidly reversed after changes in solute balance.[34] Furthermore, none of our participants were either hypernatremic (defined as [Na] > 146 mmol/L) or severely hyponatremic ([Na] < 125 mmol/L), though 13% were mild to moderately hyponatremic (125[Na]135 mmol/L). These findings may reflect transient changes related to hydration state, diet, time of day, or other factors. Most of our patients were managed as outpatients, not being ill enough to require hospital admission, and were mobile, cognitively competent outpatients with no clinical evidence of dehydration. However, plasma sodium was also associated with contrast uptake at DCE-MRI measured 1 month later, corresponding to a relative increase in nAUC in NAWM of 20% per 10 mmol/L sodium; this suggests that part of the association with brain volume may be accounted for by differences in blood volume. Age was a strong negative predictor of nAUC in GM and NAWM, consistent with literature reports of a reduction in the cerebral blood supply with age.[35] We note that, although contrast uptake in normal-appearing brain tissue is likely to be primarily intravascular, increased blood–brain barrier permeability in patients with SVD may result in an extracellular contribution to the nAUC particularly at older ages;[36] indeed, the positive association of nAUC with WMH volume may indicate such a contribution. Quantitative assessment of

Table 4. Multiple linear regression analysis of DCE-MRI measurements in normal-appearing white matter and subcortical gray matter.

	$nAUC_{GM}$ (10^{-3})		$nAUC_{NAWM}$ (10^{-3})	
	β (95% CI)	P	β (95% CI)	P
PP (mm Hg)	0.016 (−0.018, 0.050)	0.34	0.0068 (−0.022, 0.036)	0.65
MAP (mm Hg)	−0.0095 (−0.054, 0.035)	0.67	−0.0069 (−0.045, 0.032)	0.72
Hypertension	−0.44 (−1.9, 1.0)	0.55	−0.32 (−1.6, 0.93)	0.62
Salt intake score	0.14 (−0.33, 0.61)	0.56	0.015 (−0.39, 0.42)	0.94
Plasma sodium (mmol/L)	0.010 (−0.16, 0.18)	0.91	0.18 (0.030, 0.33)	0.019
Smoking	−0.36 (−1.7, 0.96)	0.59	−1.2 (−2.3, −0.034)	0.044
Stroke subtype (cortical = 0, lacunar = 1)	−0.028 (−1.2, 1.2)	0.96	−0.39 (−1.4, 0.63)	0.45
Age (years)	−0.18 (−0.24, −0.11)	<0.0001	−0.14 (−0.19, −0.082)	<0.0001
%WMH (%)	0.40 (0.0018, 0.80)	0.049	0.40 (0.053, 0.74)	0.024

Abbreviations: CI, confidence interval; DCE-MRI, dynamic contrast-enhanced magnetic resonance imaging; GM, gray matter; MAP, mean arterial pressure; nAUC, normalized area under curve; NAWM, normal-appearing white matter; PP, pulse pressure; WMH, white-matter hyperintesity.

contrast extravasation in this patient group will be considered in future work.

All analyses presented in this work were corrected for whether subjects were smokers. In line with the previous literature, smokers had both greater WMH volume[37] and lower brain volume[38] corresponding to a total brain volume difference of approximately 1% of ICV.

Our results concerning added dietary salt are limited by the qualitative and self-reported nature of these data. The index, based on a simple questionnaire, was designed for use in our clinical setting and did not attempt to assess total salt intake, an acknowledged complex task due to problems with accurate recall, and by the highly variable amounts of salt present in food or added by manufacturers during processing. However, our index may better reflect salt appetite and long-term exposure to salt. There is no gold-standard way to assess the salt intake of these patients retrospectively, and even the validity of a 24-hour urine collection, which is not practical in this cohort, has been questioned.[39] More complex questionnaires given by a dietician can provide a measure of intake but also depend on self-report and would not have been appropriate with this cohort of patients. A disadvantage of both detailed dietary questionnaires and biochemical tests is that they provide a snapshot of salt consumption, which may not reflect long-term exposure and habits, particularly during recovery from a stroke where intake may have been influenced by the recent stroke and lifestyle advice. Future work might focus on a more quantitative assessment of salt intake in patients presenting with mild stroke. Despite these reservations, our index correlated well with WMH volume and the trend was preserved when assessed using our two separate salt scores.

A second limitation is that our blood tests, while quantitative, measured plasma sodium concentration at a single point in time contemporaneous with measurement of WMH volume, %BTV, FA, and MD but not nAUC. As plasma sodium concentration shows strong individuality, it is unlikely to vary much unless the patient is over or under hydrated.[40] It should also be noted that the plasma sodium concentration can be influenced by kidney function, glucose level, and medication (13.3% of patients had reduced kidney function (estimated glomerular filtration rate $< 60\,mL/min/1.73\,m^2$) and 19.3% of patients took the diuretic medications Bendrofluimethiazide or Furosemide). However, correcting for these potential confounds made little difference to our results. Finally, we note that the age range of participants in this study was wide (34 to 96 years) and findings may be confounded by age-related effects not fully eliminated by the model; it is therefore desirable to replicate the findings in a larger study or in a sample with narrower age range.

In conclusion, arterial PP and diagnosis of hypertension predict WMH volume in patients with mild stroke. Added dietary salt intake was also independently associated with WMH. Plasma sodium concentration, while not associated with WMH volume, was a significant predictor of brain tissue volume and of gadolinium contrast agent uptake in NAWM.

Funding

The author(s) received no financial support for the research, authorship, and/or publication of this article.

Acknowledgement

This work was funded by Wellcome Trust (SDM and MRI scanning costs; grant 088134/Z/09/A), Row Fogo Charitable Trust (MCVH, AKH), Age UK (SMM), NHS Lothian

Research and Development Office (MJT), Scottish Funding Council and the Chief Scientist Office of Scotland for funding the Scottish Imaging Network: A Platform for Scientific Excellence ('SINAPSE'; JMW, radiography staff). The authors thank K Shuler for providing expert administrative support during data collection, analyses, and manuscript preparation.

Declaration of conflicting interests

The author(s) declared no potential conflicts of interest with respect to the research, authorship, and/or publication of this article.

Authors' contributions

AKH contributed to DCE-MRI analysis, statistical analysis. MJT and FMC contributed to manuscript preparation and statistical analysis. MVH contributed to processing and analysis of structural MRI and DT-MRI. PAA contributed to design of imaging protocol and to DCE-MRI and DT-MRI processing. SDM contributed to patient recruitment and assessment, collection of demographic data. SMM contributed to DT-MRI analysis. ES contributed to structural MRI analysis. PWF contributed advice regarding physiology and manuscript preparation. MSD contributed to oversight of patient clinical assessment and stroke subtyping. JMW contributed to study conception, funding and supervision, diagnostic MRI assessment, and manuscript preparation.

References

1. Aribisala BS, Morris Z, Eadie E, Thomas A, Gow A, Valdes Hernandez MC, et al. Blood pressure, internal carotid artery flow parameters, and age-related white matter hyperintensities. *Hypertension* 2014; 63: 1011–1018.
2. Maclullich AM, Ferguson KJ, Reid LM, Deary IJ, Starr JM, Seckl JR, et al. Higher systolic blood pressure is associated with increased water diffusivity in normal-appearing white matter. *Stroke* 2009; 40: 3869–3871.
3. Li XY, Cai XL, Bian PD and Hu LR. High salt intake and stroke: meta-analysis of the epidemiologic evidence. *CNS Neurosci Ther* 2012; 18: 691–701.
4. Strazzullo P, D'Elia L, Kandala NB and Cappuccio FP. Salt intake, stroke, and cardiovascular disease: meta-analysis of prospective studies. *Brit Med J* 2009; 339: b4567.
5. Decaux G. Is asymptomatic hyponatremia really asymptomatic? *Am J Med* 2006; 119: S79–S82.
6. Schrier RW. Does 'asymptomatic hyponatremia' exist? *Nat Rev Nephrol* 2010; 6: 185.
7. Bamford J, Sandercock P, Dennis M, Burn J and Warlow C. Classification and natural history of clinically identifiable subtypes of cerebral infarction. *Lancet* 1991; 337: 1521–1526.
8. Jenkinson M, Bannister P, Brady M and Smith S. Improved optimization for the robust and accurate linear registration and motion correction of brain images. *NeuroImage* 2002; 17: 825–841.
9. Hernandez MDV, Ferguson KJ, Chappell FM and Wardlaw JM. New multispectral MRI data fusion technique for white matter lesion segmentation: method and comparison with thresholding in FLAIR images. *Eur Radiol* 2010; 20: 1684–1691.
10. Filippi M and Rocca MA. Dirty-appearing white matter: a disregarded entity in multiple sclerosis. *Am J Neuroradiol* 2010; 31: 390–391.
11. Moore GR, Laule C, Mackay A, Leung E, Li DK, Zhao G, et al. Dirty-appearing white matter in multiple sclerosis: preliminary observations of myelin phospholipid and axonal loss. *J Neurol* 2008; 255: 1802–1811. (discussion 1812.
12. Valdes Hernandez Mdel C, Gallacher PJ, Bastin ME, Royle NA, Maniega SM, Deary IJ, et al. Automatic segmentation of brain white matter and white matter lesions in normal aging: comparison of five multispectral techniques. *Magn Reson Imaging* 2012; 30: 222–229.
13. Smith SM and Brady JM. SUSAN - A new approach to low level image processing. *Int J Comput Vis* 1997; 23: 45–78.
14. Farrell C, Chappell F, Armitage PA, Keston P, Maclullich A, Shenkin S, et al. Development and initial testing of normal reference MR images for the brain at ages 65–70 and 75–80 years. *Eur Radiol* 2009; 19: 177–183.
15. Patenaude B, Smith SM, Kennedy DN and Jenkinson M. A Bayesian model of shape and appearance for subcortical brain segmentation. *NeuroImage* 2011; 56: 907–922.
16. Modat M, Ridgway GR, Taylor ZA, Lehmann M, Barnes J, Hawkes DJ, et al. Fast free-form deformation using graphics processing units. *Comput Methods Programs Biomed* 2010; 98: 278–284.
17. Armitage PA, Farrall AJ, Carpenter TK, Doubal FN and Wardlaw JM. Use of dynamic contrast-enhanced MRI to measure subtle blood-brain barrier abnormalities. *Magn Reson Imaging* 2011; 29: 305–314.
18. Liu WH, Liu R, Sun W, Peng Q, Zhang WW, Xu E, et al. Different impacts of blood pressure variability on the progression of cerebral microbleeds and white matter lesions. *Stroke* 2012; 43: 2916–U253.
19. Shrestha I, Takahashi T, Nomura E, Ohtsuki T, Ohshita T, Ueno H, et al. Association between central systolic blood pressure, white matter lesions in cerebral MRI and carotid atherosclerosis. *Hypertens Res* 2009; 32: 869–874.
20. Verhaaren BFJ, Vernooij MW, de Boer R, Hofman A, Niessen WJ, van der Lugt A, et al. High blood pressure and cerebral white matter lesion progression in the general population. *Hypertension* 2013; 61: 1354–1359.
21. Waldstein SR, Wendell CR, Lefkowitz DM, Siegel EL, Rosenberger WF, Spencer RJ, et al. Interactive relations of blood pressure and age to subclinical cerebrovascular disease. *J Hypertens* 2012; 30: 2352–2356.
22. O'Rourke MF and Safar ME. Relationship between aortic stiffening and microvascular disease in brain and kidney - Cause and logic of therapy. *Hypertension* 2005; 46: 200–204.
23. Brisset M, Boutouyrie P, Pico F, Zhu YC, Zureik M, Schilling S, et al. Large-vessel correlates of cerebral small-vessel disease. *Neurology* 2013; 80: 662–669.
24. Poels MMF, Zaccai K, Verwoert GC, Vernooij MW, Hofman A, van der Lugt A, et al. Arterial stiffness and

cerebral small vessel disease The Rotterdam Scan Study. *Stroke* 2012; 43: 2637–2642.
25. Aribisala BS, Royle NA, Maniega SM, Valdes Hernandez MC, Murray C, Penke L, et al. Quantitative multi-modal MRI of the Hippocampus and cognitive ability in community-dwelling older subjects. *Cortex* 2014; 53: 34–44.
26. Mente A, O'Donnell MJ, Rangarajan S, McQueen MJ, Poirier P, Wielgosz A, et al. Association of urinary sodium and potassium excretion with blood pressure. *N Engl J Med* 2014; 371: 601–611.
27. He FJ, Li J and Macgregor GA. Effect of longer term modest salt reduction on blood pressure: Cochrane systematic review and meta-analysis of randomised trials. *Brit Med J* 2013; 346: f1325.
28. O'Donnell M, Mente A, Rangarajan S, McQueen MJ, Wang X, Liu L, et al. Urinary sodium and potassium excretion, mortality, and cardiovascular events. *N Engl J Med* 2014; 371: 612–623.
29. Cappuccio FP and Ji C. Less salt and less risk of stroke further support to action. *Stroke* 2012; 43: 1195–1196.
30. Aburto NJ, Ziolkovska A, Hooper L, Elliott P, Cappuccio FP and Meerpohl JJ. Effect of lower sodium intake on health: systematic review and meta-analyses. *BMJ* 2013; 346: f1326.
31. Gardener H, Rundek T, Wright CB, Elkind MSV and Sacco RL. Dietary sodium and risk of stroke in the Northern Manhattan Study. *Stroke* 2012; 43: 1200–1205.
32. Bragulat E, de la Sierra A, Antonio MT and Coca A. Endothelial dysfunction in salt-sensitive essential hypertension. *Hypertension* 2001; 37: 444–448.
33. Stevenson SF, Doubal FN, Shuler K and Wardlaw JM. A systematic review of dynamic cerebral and peripheral endothelial function in lacunar stroke versus controls. *Stroke* 2010; 41: e434–e442.
34. Verbalis JG. Brain volume regulation in response to changes in osmolality. *Neuroscience* 2010; 168: 862–870.
35. Aanerud J, Borghammer P, Chakravarty MM, Vang K, Rodell AB, Jonsdottir KY, et al. Brain energy metabolism and blood flow differences in healthy aging. *J Cereb Blood Flow Metab* 2012; 32: 1177–1187.
36. Farrall AJ and Wardlaw JM. Blood-brain barrier: ageing and microvascular disease—systematic review and meta-analysis. *Neurobiol Aging* 2009; 30: 337–352.
37. Staals J, Makin SD, Doubal FN, Dennis MS and Wardlaw JM. Stroke subtype, vascular risk factors, and total MRI brain small-vessel disease burden. *Neurology* 2014; 83: 1228–1234.
38. Swan GE and Lessov-Schlaggar CN. The effects of tobacco smoke and nicotine on cognition and the brain. *Neuropsychol Rev* 2007; 17: 259–273.
39. Titze J, Dahlmann A, Lerchl K, Kopp C, Rakova N, Schroder A, et al. Spooky sodium balance. *Kidney Int* 2014; 85: 759–767.
40. Zhang Z, Duckart J, Slatore CG, Fu Y, Petrik AF, Thorp ML, et al. Individuality of the plasma sodium concentration. *Am J Physiol Renal Physiol* 2014; 306: F1534–F1543.